The Journal of Eukaryotic Microbiology

ISOP Published by the International Society of Protistologists

Journal of Eukaryotic Microbiology ISSN 1066-5234

ORIGINAL ARTICLE

Morphology, Ontogeny, and Molecular Phylogeny of Two Freshwater Species of *Deviata* (Ciliophora, Hypotrichia) from Southern China

Xiaotian Luo[a], Yangbo Fan[a,b], Xiaozhong Hu[a], Miao Miao[c], Saleh A. Al-Farraj[d] & Weibo Song[a]

a Institute of Evolution and Marine Biodiversity, Ocean University of China, Qingdao 266003, China
b School of Civil and Environmental Engineering, Harbin Institute of Technology Shenzhen Graduate School, Shenzhen 518055, China
c Savaid Medical School, University of Chinese Academy of Sciences, Beijing 100049, China
d Zoology Department, King Saud University, Riyadh 11451, Saudi Arabia

Keywords
Hypotrichs; morphogenesis; SSU rRNA; Stichotrichida; taxonomy.

Correspondence
X. Hu, Institute of Evolution and Marine Biodiversity, Ocean University of China, Qingdao 266003, China
Telephone/FAX number: +86 532-8203-1610; e-mail: xiaozhonghu@ouc.edu.cn
and
M. Miao, Savaid Medical School, University of Chinese Academy of Sciences, Beijing 100049, China
Telephone/FAX number: +86 010-6967-2489; e-mail: doublemiao@126.com

Received: 20 January 2016; revised 24 April 2016; accepted May 4, 2016.

doi:10.1111/jeu.12324

ABSTRACT

The morphology and partial morphogenesis of two freshwater hypotrichous ciliates, *Deviata brasiliensis* Siqueira-Castro et al., 2009 and *Deviata rositae* Küppers et al., 2007, isolated from southern China, were investigated using live observation and protargol staining. Our populations resemble the original ones in terms of their live characters and ciliary patterns. The main determinable morphogenetic features of *D. brasiliensis* basically correspond with those of the type population. However, the origin of anlage V for either proter or opisthe is ambiguous: whether anlage V for the proter originates from parental frontoventral row 2 (the same as in the original population) or parental frontoventral row 3 (the same as in *Deviata abbrevescens*) or even de novo is not clear; the anlage V for the opisthe is possibly derived from frontoventral row 3 and further migrates to frontoventral row 2, like that in *D. abbrevescens*. In addition, the SSU rRNA gene was first sequenced for both species. Molecular phylogenetic analyses suggest that the genus *Deviata* is non-monophyletic and has a close relationship with *Perisincirra paucicirrata*.

FOR a long time, a high degree of morphological variation and adaptation and diverse morphogenetic characteristics has brought great challenges to the taxonomy of hypotrichous ciliates. However, many new inventories have been achieved from some under-sampled or insufficiently investigated biotopes in the last decade (e.g., Chen et al. 2015a; Fan et al. 2014a,b; Foissner and Stoeck 2008; Foissner et al. 2010; Gupta et al. 2006; Heber et al. 2014; Hu and Kusuoka 2015; Jung et al. 2014, 2015; Kim et al. 2014; Kumar et al. 2014, 2015; Küppers 2014; Lu et al. 2014; Luo et al. 2015; Paiva and Silva-Neto 2009; Singh and Kamra 2015). Moreover, some recent phylogenetic analyses have led to a better understanding of systematics and evolutionary relationships (e.g., Bourland 2015; Chen et al. 2014, 2015b; Fan et al. 2015; Huang et al. 2014; Lv et al. 2015; Spakova et al. 2014; Wang et al. 2015; Yi and Song 2011; Zhao et al. 2015). Among these works, only a few concern stichotrich hypotrichs (Bourland 2015; Chen et al. 2015a; Foissner et al. 2014; Jung et al. 2014; Shao et al. 2014a,b, 2015; Spakova et al. 2014).

The genus *Deviata* was established by Eigner (1995). So far, nine species have been assigned to the genus (Berger 2011; Li et al. 2014): *Deviata abbrevescens* Eigner, 1995; *Deviata bacilliformis* (Gelei, 1954) Eigner, 1995; *Deviata quadrinucleata* (Dragesco 2003) Berger, 2011; *Deviata brasiliensis* Siqueira-Castro et al., 2009; *Deviata spirostoma* (Alekperov, 1988) Berger, 2011; *Deviata polycirrata* Küppers and Claps, 2010; *Deviata rositae* Küppers et al., 2007; *Deviata estevesi* Paiva and Silva-Neto, 2005; *Deviata parabacilliformis* Li et al., 2014. Among them, only *D. bacilliformis* was redescribed (Berger 2011). The SSU rRNA gene sequence data are available only for two species: *D. bacilliformis* and *D. parabacilliformis*, and not analyzed for the type species. Therefore, the phylogenetic position of the genus is basically not resolved (Li et al. 2014).

In this article, we describe the morphology and morphogenesis of two species of *Deviata*: *D. brasiliensis* and *D. rositae*, for both of which this is the first record for China. We also first sequenced SSU rRNA gene

sequences of both species and made phylogenetic analyses.

MATERIALS AND METHODS

Morphological and morphogenetic studies

Samples were collected on 13 March 2013 (for *D. brasiliensis* and *D. rositae*) and 24 October 2013 (for *D. brasiliensis*) from Huguangyan Maar Lake (21°09′N; 110°17′E) in Guangdong Province, China. Raw cultures of all isolates were maintained in Petri dishes at about 25 °C water temperature, using habitat water with rice grains to enrich the growth of bacterial food for the ciliates. Living cells were observed in vivo using bright field and differential interference contrast microscopy and photographed using a digital camera. Protargol impregnation following the method of Wilbert (1975) was applied to reveal the infraciliature and nuclear apparatus. In vivo measurements were conducted at a magnification of 40–1,000X. Counts and measurements on stained specimens were performed at a magnification of 1,000X. Drawings of stained specimens were performed at a magnification of 1,000–1,500X with the help of a camera lucida and photomicrographs. To illustrate the changes occurring during morphogenesis, old (parental) ciliary structures are shown in outline, whereas new ones are shaded black. Terminology is according to Berger (2011).

DNA extraction, PCR amplification, and sequencing

Cells of *D. brasiliensis* and *D. rositae* were isolated and washed three times using distilled water to remove potential contamination. These cells were then transferred to a 1.5 ml microfuge tube with a minimum volume of water. Extraction of genomic DNA was performed using a DNeasy Blood & Tissue Kit (Qiagen, Hilden, Germany), following the manufacturer's instructions. PCR amplification of the SSU rRNA gene was performed using primers18s-F (5′-AACCTGGTTGATCCTGCCAGT-3′) and 18s-R (5′-TGATCCTTCTGCAGGTTCACC TAC-3′) (Medlin et al. 1988).

Phylogenetic analyses

The SSU rRNA gene sequences of *D. brasiliensis* and *D. rositae* were aligned with the sequences of 53 other hypotrichid taxa obtained from the GenBank database, with the strombidiids including *Novistrombidium orientale*, *Novistrombidium sinicum*, *Strombidinopsis jeokjo*, *Strombidinopsis acuminata*, and *Strombidium apolatum* as the outgroup taxa, using MUSCLE, which was implemented on the website http://www.ebi.ac.uk/Tools/msa/muscle/ (Edgar 2004). The accession numbers are provided after the species names in the phylogenetic tree (Fig. 7). The resulting alignment was manually edited using the program Bioedit 7.2.5 (Hall 1999), and both ends of the alignment were trimmed. The final alignment used for phylogenetic analyses included 1,756 positions and 60 taxa. Maximum likelihood (ML) analysis, with 1,000 bootstrap replicates, was carried out using RAxML-HPC2 on XSEDE v 8.1.24 (Stamatakis 2014) on the CIPRES Science Gateway with GTRGAMMA model (Miller et al. 2010). Bayesian inference (BI) analysis was performed using MrBayes 3.2.6 on XSEDE (Ronquist and Huelsenbeck 2003) on the CIPRES Science Gateway with the best-fit model GTR + I + G, which was selected by MrModeltest v2 (Nylander 2004). Markov chain Monte Carlo (MCMC) simulations were run for 10,000,000 generations with a sampling frequency of 100 and a burn-in of 25,000 trees. The remaining trees were used to calculate the posterior probabilities (PP) with a majority rule consensus. Tree topologies were visualized using Seeview v4.3.3 (Gouy et al. 2010) and MEGA 6.0 (Tamura et al. 2007). The systematic classification follows Lynn (2008) and Adl et al. (2012).

RESULTS

Chinese population of *Deviata brasiliensis* Siqueira-Castro et al., 2009

Remarks

The description is based on two populations (population I: LXT2013102406; population II: FYB2013031302) from the same sample site, and they agree in living morphology and infraciliature, especially dorsal kinety 2, which was conspicuously shortened posteriorly and composed of widely spaced bristles.

Morphological description

Cell size in vivo stable in population I, ranging within about 110–140 × 30–35 μm, while highly variable in population II: about 100–230 × 20–40 μm; body length to width ratio about 3–4:1 in population I, about 4–6:1 in population II. Body flexible, elongate, and elliptical, with both ends slightly narrowed and rounded, left and right margins more or less convex (Fig. 1A,F,G,K–O). Body almost circular in cross-section. Anterior end with conspicuous thin collar accompanied by ridges-tooth-like structures, cilia of apical membranelles emerging between these structures on dorsal side. Buccal field narrow and inconspicuous: about 20–25% of body length in population I and 15–20% of body length in population II. Cortical granules lacking. Colorless cytoplasm filled with numerous granular inclusions (approximately 1–5 μm), rendering cells opaque at low magnification in vivo (Fig. 1F–O). Contractile vacuole about 10–12 μm across, without collecting canals, located close to left body margin at about 50% of body (Fig. 1A,F,H), or slightly behind mid-body (Fig. 1K,L,N). Locomotion by moderately rapid swimming with various postures, swimming straight forward or rotating about main body axis, sometimes slowly crawling over debris with body slightly twisted.

Cells easily encyst in the absence of food in population II. Cysts usually globular and about 50 μm in diameter; cortex thin and indistinct (Fig. 1J).

Cilia of apical membranelles 10–12 μm long in vivo. All ventral cirri fine and inconspicuous in vivo, about 8 μm

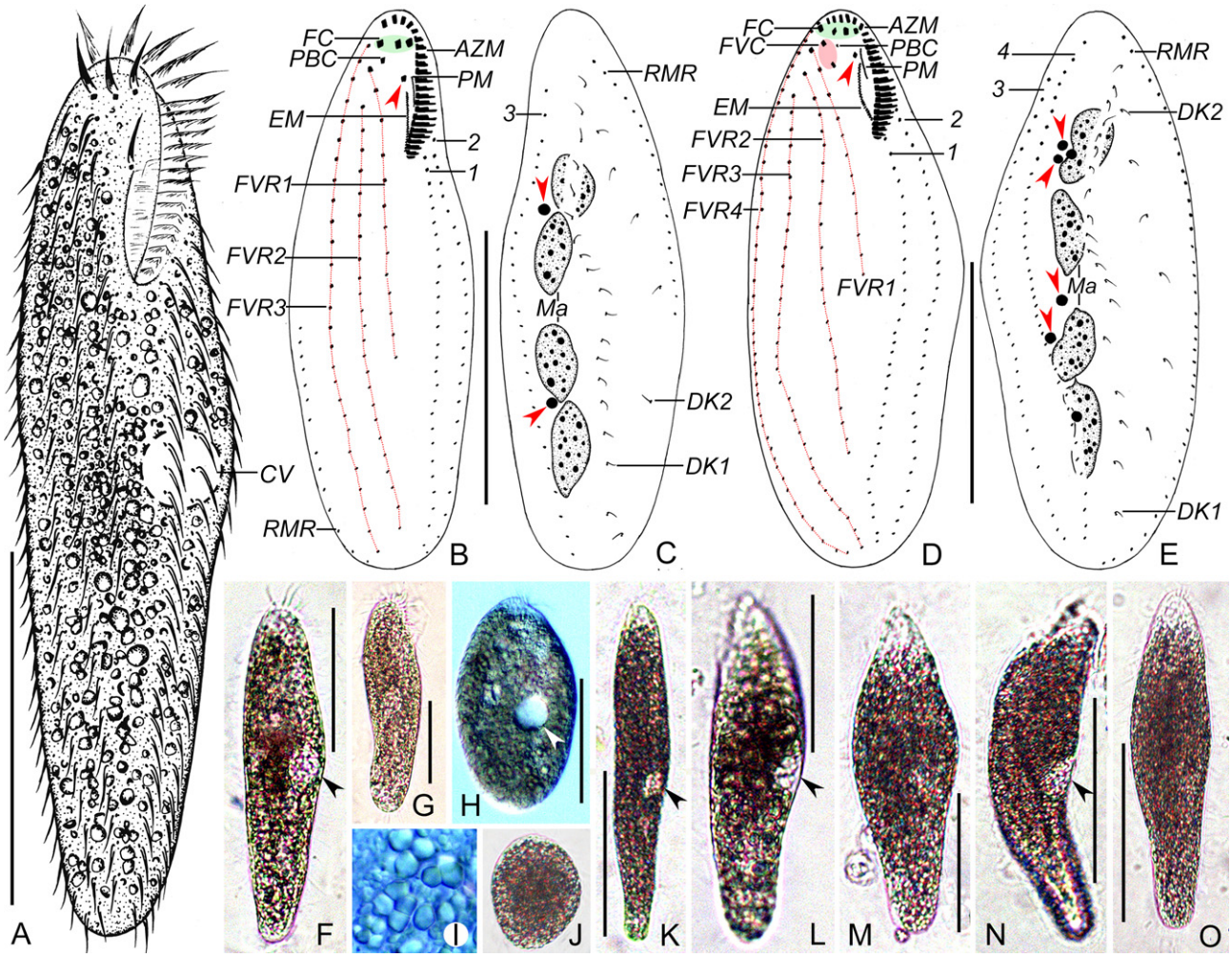

Figure 1 *Deviata brasiliensis* from life (**A, F–O**) and after protargol impregnation (**B–E**). A–I from population I, J–O from population II. (A) Ventral view of a representative individual. (B–E) Ventral (B, D) and dorsal (C, E) view, showing infraciliature and nuclear apparatus, arrowhead in B and D marks buccal cirrus, arrowheads in C and E indicate micronuclei. (F, G) Ventral views to show different body shapes, arrowhead shows contractile vacuole. (H) Ventral view of a heavily squeezed cell, showing contractile vacuole (arrowhead). (I) Cytoplasmic granules. (J) Resting cyst. (K–O) Ventral views, to show different body shapes, arrowhead shows contractile vacuole. AZM, adoral zone of membranelles; CV, contractile vacuole; DK1, 2, dorsal kinety 1, 2; EM, endoral membrane; FC, frontal cirri; FVC, frontoventral cirri; FVR1–4, frontoventral row 1–4; Ma, macronuclear segments; PBC, parabuccal cirri; PM, paroral membrane; RMR, right marginal row; 1–4, left marginal row 1–4. Scale bars = 50 μm (A–E, F–H), 100 μm (K–O).

long, except for the stronger frontal cirri, about 10–12 μm long. Most frontoventral and marginal cirri composed of two basal bodies each, except for several anterior ones composed of four basal bodies.

Infraciliature as shown in Figs. 1B–E, 2I–Q for population I and Fig. 2A–H for population II. Adoral zone of membranelles of both populations roughly in *Gonostomum* pattern (Figs. 1B,D, 2A), composed of 19–22 and 21–24 membranelles of ordinary fine-structure respectively (Table 1). Endoral membrane and paroral membrane almost straight to slightly curved, optically parallel to each other; the former long, generally multiple-rowed, the latter about half of the former in length, single-rowed, and anteriorly positioned. Three, rarely four (one out of 21 specimens investigated in population I and II, Figs. 1D, 2H), slightly enlarged frontal cirri immediately behind distal portion of adoral zone, arranged almost in a transverse pseudorow. Constantly one buccal cirrus right of anterior end of paroral membrane. Usually one, rarely two parabuccal cirri behind rightmost frontal cirrus, with the posterior one much smaller than the anterior one in population I (Figs. 1B, 2I), usually two, rarely one parabuccal cirri behind rightmost frontal cirrus in population II (Fig. 2A). One cell observed with four frontal cirri, one parabuccal cirrus, and two frontoventral cirri in population I (Fig. 1D). Usually three long frontoventral rows: frontoventral row 1 commencing slightly behind right of the parabuccal cirrus and terminating at about 60% of body length in population I,

Table 1. Morphometric data of *Deviata brasiliensis* (brI, population I; brII, population II) and *Deviata rositae* (ros) from Guangdong, China

Character[a]	Species	Min	Max	Med	Mean	SD	CV	*n*
Body, length	brI	90	129	104.0	105.1	9.9	9.5	21
	brII	113	230	188.0	182.0	30.2	16.0	20
	ros	140	267	235.0	220.5	37.9	17.2	17
Body, width	brI	30	55	38.0	39.1	6.2	15.8	21
	brII	40	84	59.5	59.1	11.0	18.4	20
	ros	23	60	34.0	36.3	10.4	28.6	17
Adoral zone, length	brI	22	27	25.0	24.3	1.6	6.7	21
	brII	28	43	33.5	34.0	3.4	10.0	21
	ros	18	34	30.0	28.6	4.2	14.7	17
Adoral membranelles, number	brI	19	22	21.0	21.0	0.8	4.0	21
	brII	21	24	22.0	22.0	0.9	4.0	20
	ros	16	21	18.0	19.0	1.3	6.6	17
Frontal cirri, number	brI	3	4	3.0	3.0	0.2	7.2	21
	brII	3	4	3.0	3.0	0.2	7.2	20
	ros	3	3	3.0	3.0	0.0	0.0	17
Buccal cirrus, number	brI	1	1	1.0	1.0	0.0	0.0	21
	brII	1	1	1.0	1.0	0.0	0.0	20
	ros	1	1	1.0	1.0	0.0	0.0	17
Parabuccal cirri, number	brI	1	2	1.0	1.3	0.5	36.0	21
	brII	1	2	2.0	1.8	0.4	20.5	20
	ros	1	2	2.0	1.6	0.5	30.8	17
Frontoventral cirri, number	brI	2	2	2.0	2.0	0.0	0.0	17
Frontoventral rows, number	brI	3	4	3.0	3.1	0.3	9.7	21
	brII	3	3	3.0	3.0	0.0	0.0	20
	ros	2	2	2.0	2.0	0.0	0.0	16
Frontoventral row 1, length	brI	50	76	61.0	60.9	7.7	12.6	21
	brII	89	167	126.0	124.5	20.8	16.5	20
	ros	83	202	150.0	146.9	34.5	23.5	16
Cirri in FVR 1, number	brI	10	21	16.0	15.6	2.3	14.5	21
	brII	13	27	21.5	21.1	3.7	17.3	20
	ros	23	37	27.0	27.5	3.8	13.9	16
Frontoventral row 2, length	brI	69	107	84.0	83.4	9.8	11.7	21
	brII	112	206	155.5	151.9	23.5	15.1	20
	ros	126	256	211.5	201.0	40.0	19.8	16
Cirri in FVR 2, number	brI	15	28	24.0	23.5	2.8	12.0	21
	brII	22	33	28.0	27.3	2.9	10.5	20
	ros	35	57	43.0	44.1	5.1	11.7	16
Frontoventral row 3, length	brI	50	125	98.0	94.3	16.8	17.8	21
	brII	127	220	173.0	171.5	24.7	14.3	20
Cirri in FVR 3, number	brI	21	38	31.0	30.8	3.8	12.5	21
	brII	29	49	37.0	37.2	4.6	12.3	20
Frontoventral row 4, length	brI	110	110	110.0	110.0	0.0	0.0	2
Cirri in FVR 4, number	brI	29	43	36.0	36.0	9.8	27.5	2
Left marginal rows, number	brI	1	5	3.0	3.0	0.9	30.1	21
	brII	2	4	3.0	2.9	2.9	10.5	20
	ros	2	3	3.0	2.7	0.5	17.8	16
Cirri in LMR 1, number	brI	16	31	25.0	23.5	4.1	17.6	21
	brII	20	39	30.5	29.2	5.0	16.4	20
	ros	26	48	32.0	34.5	6.0	17.5	16
Cirri in LMR 2, number	brI	18	33	24.0	24.9	4.4	17.6	19
	brII	21	43	33.5	32.3	6.8	20.2	20
	ros	25	45	34.0	34.6	5.8	16.6	16
Cirri in LMR 3, number	brI	19	36	27.0	27.3	4.0	14.6	15
	brII	20	46	27.0	30.8	8.2	30.4	13
	ros	34	35	34.5	34.5	0.7	2.6	11

(continued)

Table 1. (continued)

Character[a]	Species	Min	Max	Med	Mean	SD	CV	*n*
Cirri in LMR 4, number	brI	24	39	29.0	29.8	5.6	18.9	5
	brII	24	29	27.0	26.6	1.8	6.6	5
Cirri in LMR 5, number	brI	24	24	24.0	24.0	0.0	0.0	1
Cirri in RMR, number	brI	30	43	34.0	35.0	3.8	11.0	21
	brII	31	58	42.0	42.3	7.0	16.6	20
	ros	40	67	44.0	48.3	9.0	18.6	16
Dorsal kineties, number	brI	2	2	2.0	2.0	0.0	0.0	20
	brII	2	2	2.0	2.0	0.0	0.0	20
	ros	2	2	2.0	2.0	0.0	0.0	11
Dikinetids in DK 1, number	brI	15	20	17.0	17.0	0.3	7.5	20
	brII	18	28	21.0	21.4	2.5	11.0	20
	ros	15	25	20.0	19.8	3.1	15.8	11
Dikinetids in DK 2, number	brI	5	7	6.0	6.0	0.7	11.5	20
	brII	4	8	6.0	6.1	1.1	18.3	20
	ros	2	3	3.0	2.6	0.5	19.1	11
Macronuclear segments, number	brI	1	5	4.0	3.5	0.9	26.8	43
	brII	1	5	3.0	3.0	1.0	33.3	23
	ros	4	8	6.0	5.9	1.3	22.6	17
Macronuclear segment, length[b]	brI	10	54	13.0	15.3	9.0	59.0	21
	brII	14	71	26.5	31.8	14.2	53.5	20
	ros	12	33	20.0	20.8	5.6	26.8	17
Macronuclear segment, width[b]	brI	5	9	6.0	6.4	1.1	16.8	21
	brII	4	14	7.5	8.1	3.1	41.7	20
	ros	3	7	4.0	4.5	0.9	20.8	17
Micronuclei, number	brI	1	6	2.0	2.3	1.0	44.1	21
	brII	—	—	—	—	—	—	—
	ros	1	3	2.0	2.0	0.4	18.9	21
Micronucleus, length	brI	2	3	2.0	2.1	0.4	16.5	42

CV, coefficient of variation in %; DK, dorsal kinety; FVR, frontoventral row; LMR, left marginal row; Max, maximum; Mean, arithmetic mean; Med, median value; Min, minimum; *n*, number of specimens examined; RMR, right marginal row; SD, standard deviation.

[a]All data are based on protargol-impregnated specimens.

[b]Length and width of the anterior-most macronuclear segment. Measurements in μm.

and terminating at about two-thirds of body length on average in population II, some even terminating at about 85% of body length; frontoventral row 2 beginning at level of second or third cirrus of frontoventral row 1 and ending a little subterminally than frontoventral row 3 and right marginal row; frontoventral row 3 beginning almost at level of distal end of adoral zone and terminating near rear body end (Figs. 1B, 2A,N). Four long frontoventral rows observed in two of 21 specimens investigated in population I (Figs. 1D, 2M). Invariably, only one right marginal row beginning on dorsal side close to anterior end of cell, extending ventrally to the rear body end (Figs. 1B–E, 2A,B). On average three, rarely, two or four, even one or five (only one cell, Fig. 2Q) left marginal rows, becoming longer anteriorly from inside to outside with the inner one starting at the buccal vertex level (Table 1; Figs. 1B–E, 2A, B,Q).

Dorsal cilia about 3–4 μm long in vivo, arranged in two kineties: in both populations kinety 1 almost bipolar, with 15–20 and 18–28 equally spaced dikinetids, respectively; kinety 2 anteriorly and posteriorly shortened, with only 5–7 and 4–8 widely spaced dikinetids respectively (Figs. 1C,E, 2B,D,P).

Macronucleus situated left of midline, usually with four segments of variable shape, roughly ellipsoidal, ovoid, fusiform, or dumbbell-shaped (Figs. 1C,E, 2J–L,O); number of segments also unstable, ranging from one to five with variable length to width ratio (3–7:1, Fig. 2J–M). In population II some specimens with two slender segments (length to width ratio about 5–7:1 in protargol preparations, Fig. 2B,C), some with three to five segments (length to width ratio about 3:1 in protargol preparations, Fig. 2F,G), one specimen observed with only one segment (Fig. 2E).One to six, on average two, spherical micronuclei (2–3 μm in diameter) closely associated with macronuclear segments (Figs. 1C,E, 2J,L,O).

Notes on morphogenesis

Several well-impregnated dividers of different stages were found in the preparations of each population (Figs. 3C,D, G,H, 4A,B,K,M, from population I; Figs. 3A,B,E,F, 4C–J,L, from population II).

Stomatogenesis commences with the formation of the oral primordium in the opisthe, which occurs within the parental frontoventral row 1 as groups of closely spaced basal bodies (Figs. 3A, 4I). It seems that the parental

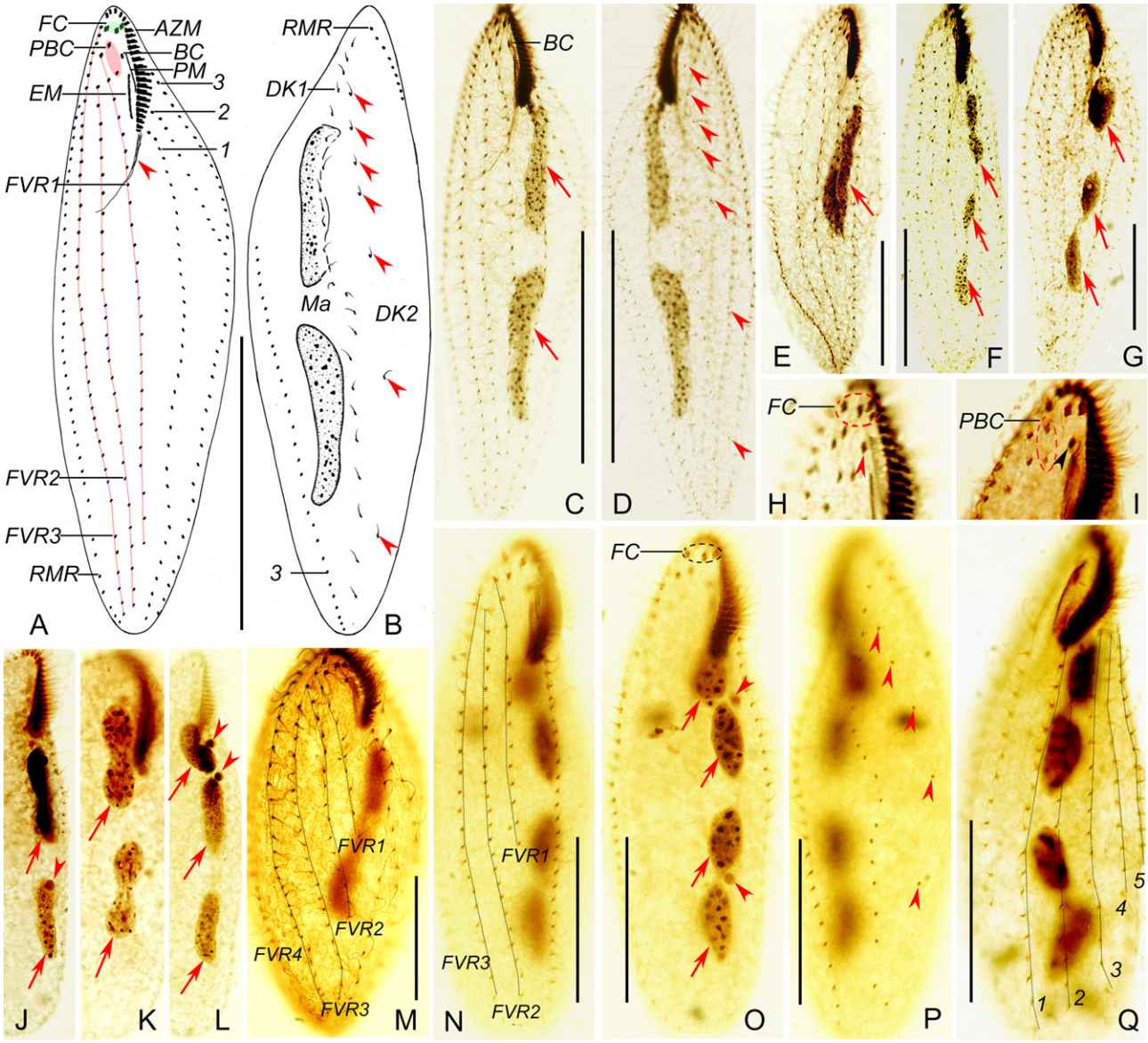

Figure 2 *Deviata brasiliensis* after protargol impregnation (**A–Q**) of population II (A–H) and I (I–Q). (A–D) Ventral (A, C) and dorsal (B, D) view of a representative specimen, showing infraciliature and nuclear apparatus, arrowhead in A marks the pharyngeal fibers, arrowheads in B and D indicate the widely spaced dikinetids of dorsal kinety 2, arrows show macronuclear segments. (E–G) Ventral views, showing variation of macronuclear segments (arrows). (H) Ventral view of anterior portion of a specimen with four frontal cirri, arrowhead marks buccal cirrus. (I) Ventral view of anterior portion of a specimen with two parabuccal cirri, arrowhead marks buccal cirrus. (J–L) Ventral views, showing different numbers and shapes of macronuclear segments (arrows) and micronuclei (arrowheads). (M) Ventral view of a specimen with four frontoventral rows and one elongate macronuclear segment. (N–P) Ventral (N, O) and dorsal (P) view of the same specimen as in Fig. 1B,C, arrows indicate macronuclear segments, arrowheads in O mark micronuclei, while in P indicate the widely spaced dikinetids of dorsal kinety 2. (Q) Ventral view of a specimen with five left marginal rows. AZM, adoral zone of membranelles; BC, buccal cirrus; DK1, 2, dorsal kinety 1, 2; EM, endoral membrane; FC, frontal cirri; FVR1–4, frontoventral row 1–4; Ma, macronuclear segments; PBC, parabuccal cirri; PM, paroral membrane; RMR, right marginal row; 1–5, left marginal row 1–5. Scale bars = 100 μm (A–D), 60 μm (E–G), 40 μm (M–Q).

structures contribute to the primordial formation. Subsequently, with the proliferation of basal bodies, the oral primordium lengthens and differentiates into new adoral membranelles in the right anterior portion (Figs. 3B–D, 4J). Then, a long primary anlage VI forms in the middle portion of the parental frontoventral row 3 (Figs. 3D, 4J).

In an early-middle divider (Fig. 3E,F), anlagen I and II of the opisthe are generated from the oral primordium. Whether anlage III forms from the parental frontoventral row 1 or the oral primordium cannot be determined. The primary anlage VI splits and forms anlage VI for both proter and opisthe. Meanwhile, the parental buccal cirrus

begins to dedifferentiate. Separate kinetids anlagen occur next to parental dikinetids on the dorsal side (arrowheads in Fig. 3F).

Then, in a middle divider (Figs. 3G,H, 4M), in the opisthe, anlage IV originates from the parental frontoventral row 2, while anlage V appears beside the parental frontoventral row 2 in the opisthe; whether it develops de novo or from frontoventral row 2 or from frontoventral row 3 and further extends to frontoventral row 2 is uncertain. At the same time, marginal cirri anlagen for the opisthe are formed within parental marginal rows. Meanwhile, in the proter, parental paroral membrane, buccal cirrus and parabuccal cirrus contribute to the construction of anlage I, II, and III, respectively; the parental endoral membrane disappear; anlage IV begins from the dedifferentiation of the anterior-most cirrus of parental frontoventral row 1; and anlage VI extends to the right of parental frontoventral row 3. On the dorsal side, two separate dorsal kinety anlagen occur within each parental kinety.

At the middle-late stage (Fig. 4A–D,G,H,K), the parental endoral membrane is resorbed entirely, and all adoral membranelles of the opisthe are formed. Anlage I forms the left frontal cirrus at its anterior end, and the posterior portion splits longitudinally into paroral and endoral membranes in both proter and opisthe; anlage II develops into the middle frontal cirrus and buccal cirrus; anlage III generates the right frontal cirrus and parabuccal cirrus/cirri. Anlage V for proter appears, the origin of which is ambiguous. Because we were not able to identify the relevant stage, we could not deduce whether anlage V in the proter develops de novo or from parental frontoventral row 2 or 3. Anlage IV for proter further extends posteriorly. Meanwhile, marginal cirri anlagen for proter are generated within the anterior portion of parental marginal rows. Dorsal kinety I anlagen lengthen and form new dikinetids in both proter and opisthe.

Finally, in a late divider (Fig. 4E,F,L), the newly built cirri and dorsal kineties move to their proper position. All parental cirri are resorbed completely at this time, except for the parental adoral zone of membranelles kept by the proter. No caudal cirri are formed.

Division of the nuclear apparatus proceeds in the usual way: macronuclear segments completely fuse into a single mass at the middle stage, and then, in the late stage, split into segments for both the proter and opisthe (Figs. 3A–D,F,H, 4B,D,F). Replication bands are present in each segment (Figs. 3A–D,F, 4I).

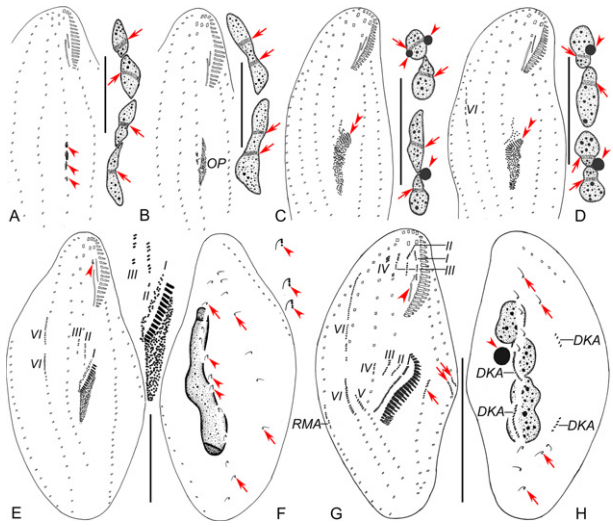

Figure 3 Morphogenesis of *Deviata brasiliensis* after protargol impregnation (**A**, **B**, **E**, **F** from population II; **C**, **D**, **G**, **H** from population I). (A–D) Ventral views of early dividers, showing replication band of macronuclear segments (arrows), oral primordium of the opisthe, and anlage VI, arrowheads in A mark the closely spaced basal bodies of the oral primordium, while in C and D indicate micronuclei, double arrowheads mark the new adoral membranelles. (E, F) Ventral (E) and dorsal (F) view of an early-middle divider, showing anlagen I–III, VI, and the dedifferentiation of parental buccal cirrus (arrowhead in E), arrows in F indicate the old dikinetids, arrowheads in F mark the newly formed kinetids (inset) within dorsal kinety 1. (G, H) Ventral (G) and dorsal (H) view of a middle divider, arrows in G indicate the left marginal rows anlagen for the opisthe, while in H mark the old dikinetids, arrowhead in G shows the old endoral membrane, while in H indicates the micronucleus. DKA, dorsal kinety anlagen; OP, oral primordium of the opisthe; RMA, right marginal row anlage; I–VI, frontoventral anlagen I–VI. Scale bars = 40 μm.

Deposition of voucher slides

Four voucher slides from population I (registration no. LXT2013102406/1–4) and two voucher slides from population II (registration no. FYB2013031302/1–2) have been deposited in the Laboratory of Protozoology, Ocean University of China, Qingdao, China.

Ecology

Water temperature was 25 and 27 °C and pH was 8.2.

Chinese population of *Deviata rositae* Küppers et al., 2007

Morphological description

Body in life about 200–300 × 15–25 μm; vermiform, very slender with length to width ratio about 7–10:1 in vivo and 6:1 on average after fixation. Body almost round in cross-section, anterior portion slightly dorsoventrally flattened. Cell very flexible, but not contractile (Fig. 5A,J–O). Buccal field narrow and inconspicuous, about 10% of body length. Cortical granules not recognizable. Cytoplasm colorless, filled with lipid inclusions with variable size, approximately 1–5 μm, rendering cells opaque except for the transparent anterior portion of the cell (Fig. 5J–P). Contractile vacuole positioned close to left body margin in about anterior one-third of body length, about 7 μm across (Fig. 5A). Locomotion by slowly swimming in water, rotating about main body axis, sometimes slowly crawling over debris with body obviously twisted.

Adoral zone of membranelles roughly in *Gonostomum*-pattern, composed of 16–21 membranelles with only three distal ones located at anterior end of the cell (Fig. 5B). Paroral membrane and endoral membrane almost straight, and parallel to each other; the

former, generally single-rowed, located ahead of the latter, which is multiple-rowed and longer (Fig. 5F,G). Pharyngeal fibers conspicuous in stained specimens, ca. 40 μm long, extending obliquely backwards (Fig. 5B). Constantly three slightly enlarged frontal cirri arranged almost in a pseudorow; one buccal cirrus located anterior of endoral membrane (Fig. 5F,G). One or two parabuccal cirri distributed behind right frontal cirrus (Fig. 5B). Invariably two long frontoventral rows: row 1 commencing slightly behind right of parabuccal cirri and terminating about two-thirds of body length; row 2 beginning close to anterior end of cell and ending just a little subterminally to the right marginal row (Fig. 5B). One right marginal row beginning dorsolaterally and extending nearly to posterior end of the cell on ventral side. Two or three left marginal rows, the inner row commencing close to the rear end of the adoral zone and terminating at the rear end of the body; the middle and outer rows beginning a little anterior to the inner row, usually extending onto dorsolateral side posteriorly (Table 1). All cirri fine, most frontoventral and marginal cirri composed of two basal bodies each, except for a few in anterior portion composed of four basal bodies.

Dorsal cilia about 3–4 μm long in vivo, arranged in two kineties of different length: kinety 1 almost bipolar, with dikinetids densely spaced anteriorly and widely spaced posteriorly; kinety 2 (very likely dorsomarginal kinety) composed of two or three dikinetids only (Fig. 5C,H,I).

Macronucleus moniliform, composed of 4–8 ellipsoidal segments connected by a fine strand, located left of midline (Fig. 5C,D). One to three, on average two, spherical micronuclei (2–3 μm in diameter) closely associated with macronuclear segments (Fig. 5D,E).

Notes on morphogenesis

Only one middle divider, which shows some details of this part of the life cycle, was found in preparations (Fig. 6A–D). Frontoventral anlagen I–VI, marginal anlagen, and dorsal kinety anlagen for the proter and opisthe were all formed. All the macronuclear segments completely fused into a single mass at this stage. Some morphogenetic characters can be deduced as follows: marginal rows develop in the ordinary manner, that is, by intrakinetal proliferation within each row in both proter and opisthe; anlage for dorsal kinety 1 may occur within parental dorsal kinety 1. The anlagen of dorsal kinety 2 are closely located to the anlagen of the right marginal row. Due to the lack of other division stages in our preparations, we were not able to determine the origins of the anlagen of dorsal kinety 2, or of the adoral zone of membranelles in the proter. Likewise, the exact origin of the frontoventral anlagen I–VI and of the oral primordium remains unclear.

Deposition of voucher slides

Three voucher slides (registration no. FYB2013031303/1–3) have been deposited in the Laboratory of Protozoology, Ocean University of China, Qingdao, China.

Ecology

Water temperature was 27 °C and pH was 8.2.

SSU rRNA gene sequence and phylogenetic analyses

The SSU rRNA gene sequence of *D. brasiliensis* (population I, GenBank accession number KP266620) is 1,695 bp long and has a G+C content of 44.90 mol%, while that of *D. rositae* (GenBank accession number KU525298) is 1,730 bp long and has a G+C content of 45.09 mol%. Two populations of *D. brasiliensis* share 100.0% sequence similarity. Sequence similarities between species of the genus *Deviata* and *Perisincirra* are shown in Table 2.

The topologies of the BI and ML trees inferred from SSU rRNA gene sequences were basically congruent with variable support values; therefore, only the BI topology (with nodal support from both methods) is shown (Fig. 7). The phylogenetic analyses showed that four *Deviata* species and *Perisincirra paucicirrata* cluster in a clade, in which *D. rositae* and *D. parabacilliformis* cluster together with relatively high support (0.99 BI, 86% ML). The latter two species are sister to another group comprising *D. brasiliensis*, *D. bacilliformis*, and *P. paucicirrata*.

DISCUSSION

Comparison of Chinese populations of *Deviata brasiliensis* with type population and with congeners

Morphologically, our populations correspond well with the population described by Siqueira-Castro et al. (2009), such as the body shape, contractile vacuole, the variable number of macronuclear segments, especially the ciliary pattern, and dorsal kinety 2 with widely spaced bristles. The type population mainly differs from our populations as follows: the anterior cirri of the frontoventral row 1 were misaligned (in about 60% of the specimens investigated vs. none in our populations). Some interphase specimens with misaligned cirri may be caused by the fragment of anlage IV, which should not be considered as an interspecific difference. Some other minor differences lie in the following aspects: the type population having a somewhat smaller body than population II (110 × 45 μm in vivo and 62–160 × 28–64 μm after protargol impregnation vs. 100–230 × 20–40 μm in vivo and 113–230 × 40–84 μm after protargol impregnation), but a similar body size with population I (110–140 × 30–35 μm in vivo and 90–129 × 30–55 μm after protargol impregnation); variable number of adoral membranelles (18–31 vs. 19–22 in population I and 21–24 in population II); more left marginal rows (3–6 vs. 1–5 in population I and 2–4 in population II). However, these variations can be considered as population dependent because limnetic and terrestrial ciliates in different habitats can have variable body sizes (Foissner et al. 2002), and thus these populations are conspecific.

In terms of the similar ciliary pattern, especially dorsal kinety 2 with widely spaced bristles, the type species *D. abbrevescens* should be compared with our populations of *D. brasiliensis*. However, the former differs from

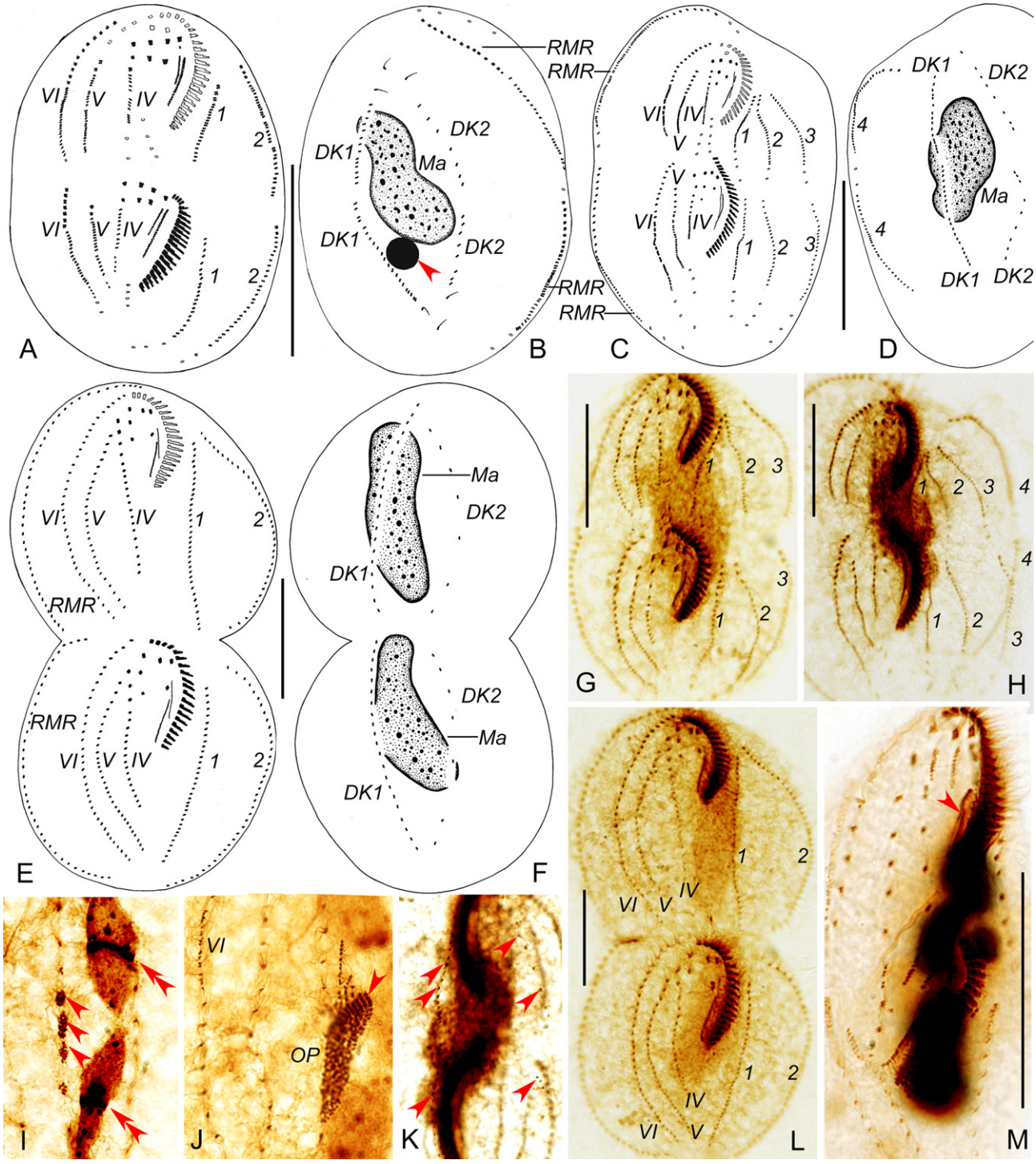

Figure 4 Morphogenesis of *Deviata brasiliensis* after protargol impregnation (**A**, **B**, **K**, **M** from population I; **C–J**, **L** from population II). (A–D) Ventral (A, C) and dorsal (B, D) views of middle-late dividers, arrowhead indicates micronucleus. (E, F) Ventral (E) and dorsal (F) view of a late divider, showing nearly completion of cirral development. (G, H) Ventral views of middle-late dividers, showing 3 (E) and 4 (F) left marginal cirri anlagen respectively. (I) Portion of an early divider, showing closely spaced basal bodies of the oral primordium (arrows) and replication band (double arrowheads) of macronuclear segments. (J) Detail of an early stage, showing the newly formed adoral membranelles (arrowhead) and primary frontoventral anlagen VI. (K) Dorsal view showing the newly formed dikinetids (arrowheads). (L) Ventral view of a late divider, the same specimen as E. (M) Ventral view of a middle divider, the same as in Fig. 3G, arrowhead marks the old endoral membrane. DK1, 2, the newly formed dorsal kinety 1, 2; Ma, macronuclear segments; OP, oral primordium of the opisthe; RMR, the newly formed right marginal row; IV–VI, frontoventral anlagen IV–VI; 1–4, left marginal row anlage 1–4. Scale bars = 40 μm.

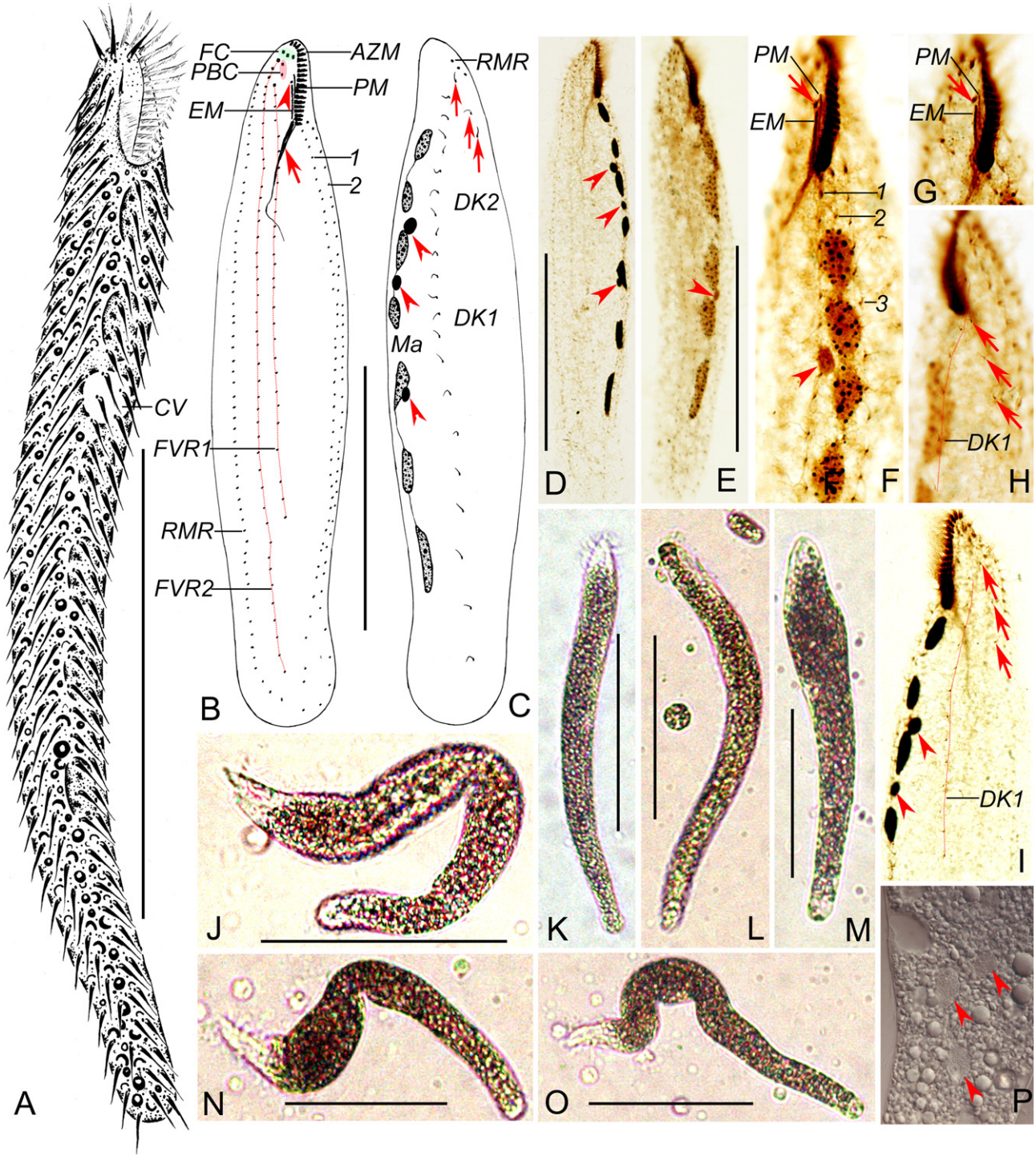

Figure 5 *Deviata rositae* from life (**A**, **J–P**) and after protargol impregnation (**B–I**). (A) Ventral view of a representative individual. (B–D) Ventral (B, D) and dorsal (C) view of a typical specimen, showing infraciliature and nuclear apparatus, arrowhead in B indicates buccal cirrus, arrowheads in C and D mark micronuclei, arrow in B indicates the conspicuous pharyngeal fibers, arrows in C show the dikinetids of dorsal kinety 2. (E) Ventral view of a specimen with six macronuclear segments and one micronucleus (arrowhead). (F, G) Ventral views of the anterior part, showing the detail of the undulating membranes and the buccal cirrus (arrow), arrowhead indicates the micronucleus. (H, I). Detail showing dorsal kineties, arrows mark the dikinetids of dorsal kinety 2, arrowheads indicate micronuclei. (J–O) Ventral views, to show different body shapes and flexibility of cells. (P) Macronuclear segments (arrowheads) and cytoplasmic granules. AZM, adoral zone of membranelles; CV, contractile vacuole; DK1, 2, dorsal kinety 1, 2; EM, endoral membrane; FC, frontal cirri; FVR1, 2, frontoventral cirri row 1, 2; Ma, macronuclear segments; PBC, parabuccal cirri; PM, paroral membrane; RMR, right marginal row; 1–3, left marginal row 1–3. Scale bars = 100 μm.

our populations in having more parabuccal cirri (2–9, 4 on average, vs. 1–2, 1.3 on average, in population I; 1–2, 1.8 on average, in population II), two long rod-shaped macronuclear segments (vs. 1–5, 3.5 or 3 segments on average, with variable shapes for population I and II), and a higher number of basal bodies forming most of the somatic cirri (4 vs. 2) (Eigner 1995).

The main morphogenetic features of our populations correspond well with those of the type population: (i) six frontoventral anlagen are present; (ii) in the opisthe, the oral primordium, anlagen I and II (maybe including anlage III) are derived from the same anlage, which originated from parental frontoventral row 1, and anlage IV is generated from parental frontoventral row 2; (iii) in the proter, anlage I, II, and III originate from the parental paroral, the buccal cirrus, and the parabuccal cirrus/cirri, respectively, and anlage IV is formed from parental frontoventral row 1 and further extends to frontoventral row 2; (iv) the long primary anlage VI splits and forms anlage VI for the proter and opisthe; (v) the left and right marginal rows and the dorsal kineties develop intrakinetally; (vi) no parental cirral rows are retained after division, except for the parental adoral zone of membranelles kept by the proter; and (vii) and all macronuclear nodules fuse into a single mass and then divide (Siqueira-Castro et al. 2009).

However, the origin of anlage V for either the proter or opisthe is ambiguous in Chinese populations. Whether anlage V for the proter originates from parental frontoventral row 2 (as in the original population of *D. brasiliensis*) or parental frontoventral row 3 (as in *D. abbrevescens*) or even de novo is not clear. The origin of anlage V for the opisthe is not unambiguously determined for the original population just as our populations. It is more likely that the anlage V for the opisthe originates from frontoventral row 3 and further deviates to frontoventral row 2, which is the same as that in *D. abbrevescens*. The origin of anlage IV is of the *D. abbrevescens* type (originating in parental frontoventral row 1 and further extending into parental frontoventral row 2), which may also be the same as the original population of *D. brasiliensis* (the only mentioned anlage IV forming from parental frontoventral row 1) (Eigner 1995; Siqueira-Castro et al. 2009).

Comparison of Chinese population of *Deviata rositae* with type population

Our population possesses most of the diagnostic features described by Küppers et al. (2007), especially only two long frontoventral rows as well as one long and one short dorsal kinety. Compared with our form, the original population is smaller (112–154 × 21–28 μm in vivo and 98–154 × 25–56 μm after protargol impregnation vs. 200–300 × 15–25 μm in vivo and 140–267 × 23–60 μm after protargol impregnation) and has a little more macronuclear segments (7–14, 9 on average, vs. 4–8, 6 on average) and fewer cirri (Küppers et al. 2007). However, these differences can be considered as population-dependent, owing to the variation of body size of limnetic and terrestrial ciliates (Foissner et al. 2002).

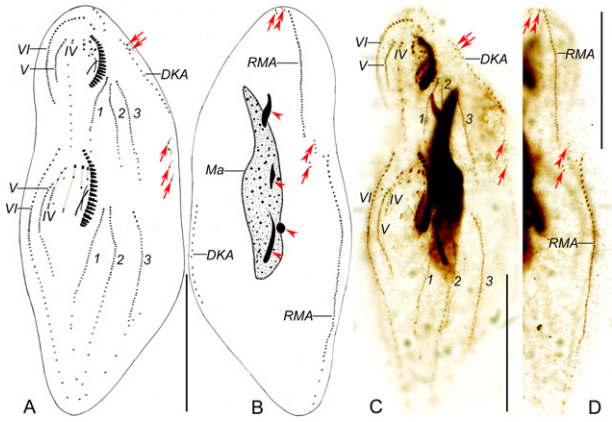

Figure 6 A middle divider of *Deviata rositae* after protargol impregnation (**A–D**). (A–D) Ventral (A, C) and dorsal (B, D) views of the same specimen, arrows in A and C show the old dikinetids of dorsal kinety 1, while in B and D indicate the newly formed dikinetids of dorsal kinety 2, double arrowheads indicate the old right marginal cirri, arrowheads mark the dividing micronuclei. DKA, dorsal kinety anlagen; Ma, macronuclear segments; RMA, right marginal row anlage; IV–VI, frontoventral anlagen IV–VI; 1–3, left marginal row anlage 1–3. Scale bars = 40 μm.

Some ontogenetic data are lacking; therefore, the exact origin of the various frontoventral anlagen is not definite. One middle divider indicates that this species possesses six frontoventral anlagen like its congeners. The origin of the short dorsal kinety 2 is unclear.

Systematic positions of genera *Deviata* and *Perisincirra*

Eigner (1995) established *Deviata* and classified it in the family Kahliellidae without giving a detailed explanation. Subsequently, Eigner (1997) reclassified the genus in the family Oxytrichidae as a supposed ancestor of Oxytrichidae. Nevertheless, Lynn and Small (2002), Jankowski (2007), Küppers et al. (2007), and Lynn (2008) took over the original classification of *Deviata* in Kahliellidae. Berger (2011) was uncertain about the phylogenetic position of *Deviata* and treated it as a non-dorsomarginalian hypotrich.

Unlike the oxytrichids, *Deviata* lacks dorsomarginal kineties and dorsal kinety fragmentation, strongly

Table 2. Sequence similarities between species of the genus *Deviata* and *Perisincirra*

Sequence similarity	D.br	D.ro	D.ba	D.pa	P.pa
D.br	—	0.988	0.983	0.984	0.991
D.ro	0.988	—	0.983	0.990	0.984
D.ba	0.983	0.983	—	0.979	0.989
D.pa	0.984	0.990	0.979	—	0.981
P.pa	0.991	0.984	0.989	0.981	—

D.ba, *Devitata bacilliformis*; D.br, *Deviata brasiliensis*; D.pa, *Deviata parabacilliformis;* D.ro, *Deviata rositae*; P.pa, *Perisincirra paucicirrata*.

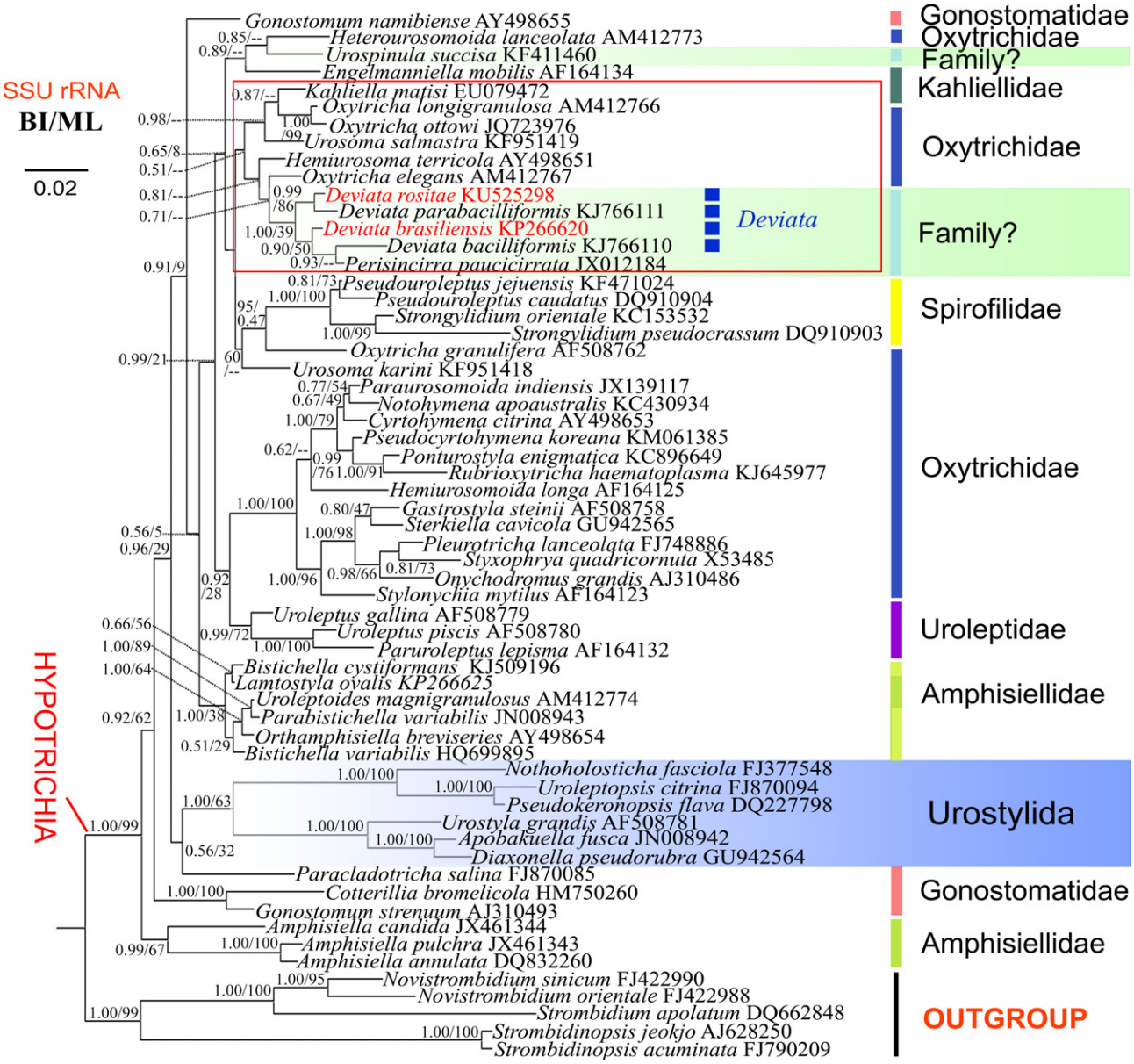

Figure 7 The Bayesian inference (BI) tree inferred from the small subunit ribosomal RNA (SSU rRNA) gene sequences, showing the position of *Deviata brasiliensis* and *Deviata rositae* (indicated in red). Numbers near branches denote posterior probability value for BI and bootstrap values for ML. "—" indicates topologies that differ in the ML and BI phylogenies. All branches are drawn to scale. Scale bar corresponds to two substitutions per 100 nucleotide positions. GenBank accession numbers are given for each species.

indicating that it does not belong to the dorsomarginalian hypotrichs and should not be included in the family Oxytrichidae. It is widely accepted that the kahlidellids retain some parental cirral rows after division, which is, however, absent in all known *Deviata* species; therefore, the classification of *Deviata* in the family Kahliellidae is incorrect (Berger 2011). In the current phylogenetic analysis, *Deviata* species cluster in different clades than *Kahliella*, the name-bearing type of the Kahliellidae, which also rejects the inclusion of *Deviata* in the Kahliellidae.

The phylogenetic analyses based on SSU rRNA genes show that the four *Deviata* species have a close relationship with *P. paucicirrata*, which is consistent with their morphological similarities: both with the adoral zone of membranelles and even undulating membranes roughly in *Gonostomum* pattern; with more than one cirral rows right and left of midline; three frontal cirri; buccal, and parabuccal cirrus/cirri present; frontoterminal, postoral ventral, pretransverse ventral, and transverse cirri lacking; typical parental (old) cirral rows absent. However, the former differs from the later mainly in the much more densely

spaced cirri and the absence of caudal cirri. According to Li et al. (2013), *P. paucicirrata* has four frontoventral anlagen, of which the long right and left rows are all marginal rows; that is, there are no long frontoventral rows (vs. having six frontoventral anlagen with more than two long frontoventral rows of *Deviata*) (Dragesco 2003; Eigner 1995, 1997; Küppers and Claps 2010; Küppers et al. 2007; Siqueira-Castro et al. 2009).

Owing to the lack of retained parental cirral rows, *Perisincirra* also cannot be classified in the family Kahliellidae, just the same as *Deviata*. However, since molecular data are not available for the type species of *Kahliella*, *Deviata,* and *Perisincirra* (*K. acrobates*, *D. abbrevescens,* and *P. kahli*), respectively, any conclusion on a definite familial assignment of these genera would be premature. Due to the low sequence divergence in this group of ciliates, the SSU rRNA gene may not be well-suited to infer the true phylogenetic relationships. Additional molecular data (e.g., multigene of type species and more other species) and more detailed ontogenetic information are needed.

ACKNOWLEDGMENTS

This work was supported by the National Natural Science Foundation of China (Project numbers: 31430077, 31522051), the Deanship of Scientific Research at King Saud University for its funding this Prolific Research Group (PRG-1436-24), the Applied Basic Research Plan of Qingdao (15-12-1-1-jch) and the Science Foundation of the Chinese Academy of Sciences (KJRH2015-013). We would like to thank Ms. Chundi Wang (OUC) for gene sequencing, and Prof. Xiaofeng Lin, Southern China Normal University, for ensuring institutional support for this research.

LITERATURE CITED

Adl, S. M., Simpson, A. G. B., Lane, C. E., Lukeš, J., Bass, D., Bowser, S. S., Brown, M. W., Burki, F., Dunthorn, M., Hampl, V., Heiss, A., Hoppenrath, M., Lara, E., Gall, L. L., Lynn, D. H., Mcmanus, H., Mitchell, E. A. D., Mozley-Stanridge, S. E., Parfrey, L. W., Pawlowski, J., Rueckert, S., Shadwick, L., Schoch, C. L., Smirnov, A. & Spiegel, F. W. 2012. The revised classification of eukaryotes. *J. Eukaryot. Microbiol.*, 59:429–493.

Alekperov, I. K. 1988. Two new species of infusoria (Ciliophora, Hypotrichida) from fresh waters of Azerbaijan. *Zool. Zh.*, 67:777–780 (in Russian with English summary).

Berger, H. 2011. Monograph of the Gonostomatidae and Kahliellidae (Ciliophora, Hypotricha). *Monogr. Biol.*, 90:1–741.

Bourland, W. A. 2015. Morphology, ontogenesis and molecular characterization of *Atractos contortus* Vörösváry, 1950 and *Stichotricha aculeata* Wrzesniowskiego, 1866 (Ciliophora, Stichotrichida) with consideration of their systematic positions. *Eur. J. Protistol.*, 51:351–373.

Chen, X., Miao, M., Ma, H., Al-Rasheid, K. A. S., Xu, K. & Lin, X. 2014. Morphology, ontogeny, and phylogeny of two brackish urostylid ciliates (Protist, Ciliophora, Hypotricha). *J. Eukaryot. Microbiol.*, 61:594–610.

Chen, L., Zhao, X., Ma, H., Warren, A., Shao, C. & Huang, J. 2015a. Morphology, morphogenesis and molecular phylogeny of a soil ciliate, *Pseudouroleptus caudatus caudatus* Hemberger, 1985 (Ciliophora, Hypotricha), from Lhalu Wetland, Tibet. *Eur. J. Protistol.*, 51:1–14.

Chen, X., Zhao, X., Liu, X., Warren, A., Zhao, F. & Miao, M. 2015b. Phylogenomics of non-model ciliates based on transcriptomic analyses. *Protein Cell*, 6:373–385.

Dragesco, J. 2003. Infaciliature et morphometrie de vingt espèces de ciliés hypotriches recoltés au Rwanda et Burundi, comprenant *Kahliella quadrinucleata* n. sp. *Pleurotricha multinucleata* n. sp. et *Laurentiella bergeri* n. sp. *Trav. Mus. Natl. Hist. Nat. Grigore Antipa*, 45:7–59.

Edgar, R. C. 2004. Muscle: multiple sequence alignment with high accuracy and high throughput. *Nucleic Acids Res.*, 32:1792–1797.

Eigner, P. 1995. Divisional morphogenesis in *Deviata abbrevescens* nov. gen., nov. spec., *Neogeneia hortualis* nov. gen., nov. spec., and *Kahliella simplex* (Horvath) Corliss and redefinition of the Kahliellidae (Ciliophora, Hypotrichida). *Eur. J. Protistol.*, 31:341–366.

Eigner, P. 1997. Evolution of morphogenetic processes in the Orthoamphisiellidae n. fam., Oxytrichidae, and Parakahliellidae n. fam., and their depiction using a computer method (Ciliophora, Hypotrichida). *J. Eukaryot. Microbiol.*, 44:553–573.

Fan, Y., Chen, X., Hu, X., Shao, C., Al-Rasheid, K. A. S., Al-Farraj, S. A. & Lin, X. 2014a. Morphology and morphogenesis of *Apoholosticha sinica* n. g., n. sp. (Ciliophora, Hypotrichia), with consideration of its systematic position among urostylids. *Eur. J. Protistol.*, 50:78–88.

Fan, Y., Pan, Y., Huang, J., Lin, X., Hu, X. & Warren, A. 2014b. Molecular phylogeny and taxonomy of two novel brackish water hypotrich ciliates, with the establishment of a new genus, *Antiokeronopsis* gen. n. (Ciliophora, Hypotrichia). *J. Eukaryot. Microbiol.*, 61:449–462.

Fan, Y., Zhao, X., Hu, X., Miao, M., Warren, A. & Song, W. 2015. Taxonomy and molecular phylogeny of two novel ciliates, with establishment of a new genus, *Pseudogastrostyla* n. g. (Ciliophora, Hypotrichia, Oxytrichidae). *Eur. J. Protistol.*, 51:374–385.

Foissner, W., Agatha, S. & Berger, H. 2002. Soil ciliates (Protozoa, Ciliophora) from Namibia (Southwest Africa), with emphasis on two contrasting environments, the Etosha region and the Namib Desert. *Denisia*, 5:1–1459.

Foissner, W., Filker, S. & Stoeck, T. 2014. *Schmidingerothrix salinarum* nov. spec. is the molecular sister of the large oxytrichid clade (Ciliophora, Hypotricha). *J. Eukaryot. Microbiol.*, 61:61–74.

Foissner, W., Shi, X., Wang, R. & Warren, A. 2010. A reinvestigation of *Neokeronopsis* populations, including the description of *N. asiatica* nov. spec. (Ciliophora, Hypotricha). *Acta Protozool.*, 49:87–105.

Foissner, W. & Stoeck, T. 2008. Morphology, ontogenesis and molecular phylogeny of *Neokeronopsis* (*Afrokeronopsis*) *aurea* nov. subgen., nov. spec. (Ciliophora: Hypotricha), a new African flagship ciliate confirms the CEUU hypothesis. *Acta Protozool.*, 47:1–33.

Gelei, J. 1954. Über die Lebensgemeinschaft einiger temporärer Tümpel auf einer Bergwiese im Börzsönygebirge (Oberungarn) III. *Ciliaten. Acta boil. Hung.*, 5:259–343.

Gouy, M., Guindon, S. & Gascuel, O. 2010. SeaView version 4: a multiplatform graphical user interface for sequence alignment and phylogenetic tree building. *Mol. Biol. Evol.*, 27:221–224.

Gupta, R., Kamra, K. & Sapra, G. R. 2006. Morphology and cell division of the Oxytrichids *Architricha indica* nov. gen., nov. sp., and *Histriculus histrio* (Müller, 1773), Corliss, 1960 (Ciliophora, Hypotrichida). *Eur. J. Protistol.*, 42:29–48.

Hall, T. A. 1999. BioEdit: a user-friendly biological sequence alignment editor and analysis program for Windows 95/98/NT. *Nucleic Acids Symp.*, 41:95–98.

Heber, D., Stoeck, T. & Foissner, W. 2014. Morphology and ontogenesis of *Psilotrichides hawaiiensis* nov. gen., nov. spec. and

molecular phylogeny of the Psilotrichidae (Ciliophora, Hypotrichia). *J. Eukaryot. Microbiol.*, 61:260–277.

Hu, X. & Kusuoka, Y. 2015. Two oxytrichids from the ancient Lake Biwa, Japan, with notes on morphogenesis of *Notohymena australis* (Ciliophora, Sporadotrichida). *Acta Protozool.*, 54:107–122.

Huang, J., Chen, Z., Song, W. & Berger, H. 2014. Three-gene based phylogeny of the Urostyloidea (Protista, Ciliophora, Hypotricha), with notes on classification of some core taxa. *Mol. Phylogenet. Evol.*, 70:337–347.

Jankowski, A. V. 2007. Phylum Ciliophora Doflein, 1901. Review of taxa. *In:* Alimov, A. F. (ed.), Protista: Handbook on Zoology, Vol. Part 2. Nauka, St Petersburg. p. 415–993. (in Russian with English summary).

Jung, J. H., Park, K. M. & Min, G. S. 2014. Morphology and molecular phylogeny of *Pseudouroleptus jejuensis* nov. spec., a new soil ciliate (Ciliophora, Spirotrichea) from South Korea. *Acta Protozool.*, 53:195–206.

Jung, J. H., Park, K. M. & Min, G. S. 2015. Morphology and molecular phylogeny of *Pseudocyrtohymena koreana* n. g., n. sp. and Antarctic *Neokeronopsis asiatica* Foissner et al. 2010 (Ciliophora, Sporadotrichida), with a brief discussion of the *Cyrtohymena* undulating membranes pattern. *J. Eukaryot. Microbiol.*, 62:280–297.

Kim, J. H., Vdacny, P., Shazib, S. U. & Shin, M. K. 2014. Morphology and molecular phylogeny of *Apoterritricha lutea* n. g., n. sp. (Ciliophora, Spirotrichea, Hypotrichia): a putative missing link connecting *Cyrtohymena* and *Afrokeronopsis*. *J. Eukaryot. Microbiol.*, 61:520–536.

Kumar, S., Bharti, D., Marinsalti, S., Insom, E. & Terza, A. L. 2014. Morphology, morphogenesis, and molecular phylogeny of *Paraparentocirrus sibillinensis* n. gen., n. sp., a "Stylonychine Oxytrichidae" (Ciliophora, Hypotrichida) without transverse cirri. *J. Eukaryot. Microbiol.*, 61:247–259.

Kumar, S., Kamra, K., Bharti, D., Terza, A. L., Sehgal, N., Warren, A. & Sapra, G. R. 2015. Morphology, morphogenesis, and molecular phylogeny of *Sterkiella tetracirrata* n. sp. (Ciliophora, Oxytrichidae), from the Silent Valley National Park, India. *Eur. J. Protistol.*, 51:86–97.

Küppers, G. 2014. Morphology of *Clapsiella magnifica* gen. n., sp. n., a new hypotrichous ciliate with a curious dorsal ciliary pattern. *Eur. J. Protistol.*, 50:373–381.

Küppers, G. & Claps, M. C. 2010. Morphology and notes on morphogenesis during cell division of *Deviata polycirrata* n. sp. and of *Deviata bacilliformis* (Ciliophora: Kahliellidae) from Argentina. *J. Eukaryot. Microbiol.*, 57:273–284.

Küppers, G., Lopretto, E. C. & Claps, M. C. 2007. Description of *Deviata rositae* n. sp., a new ciliate species (Ciliophora, Stichotrichia) from Argentina. *J. Eukaryot. Microbiol.*, 54:443–447.

Li, F., Lv, Z., Yi, Z., Al-Farraj, S. A., Al-Rasheid, K. A. S. & Shao, C. 2014. Taxonomy and phylogeny of two species of the genus *Deviata* (Protista, Ciliophora) from China, with description of a new soil form, *Deviata parabacilliformis* sp. nov. *Int. J. Syst. Evol. Microbiol.*, 64:3775–3785.

Li, F., Xing, Y., Li, J., Al-Rasheid, K. A. S., He, S. & Shao, C. 2013. Morphology, morphogenesis and small subunit rRNA gene sequence of a soil hypotrichous ciliate, *Perisincirra paucicirrata* (Ciliophora, Kahliellidae), from the shoreline of the Yellow River, North China. *J. Eukaryot. Microbiol.*, 60:247–256.

Lu, X., Gao, F., Shao, C., Hu, X. & Warren, A. 2014. Morphology, morphogenesis and molecular phylogeny of a new marine ciliate, *Trichototaxis marina* n. sp. (Ciliophora, Urostylida). *Eur. J. Protistol.*, 50:524–537.

Luo, X., Gao, F., Al-Rasheid, K. A. S., Warren, A., Hu, X. & Song, W. 2015. Redefinition of the hypotrichous ciliate *Uncinata*, with descriptions of the morphology and phylogeny of three urostylids (Protista, Ciliophora). *Syst. Biodivers.*, 13:455–471.

Lv, Z., Shao, C., Yi, Z. & Warren, A. 2015. A molecular phylogenetic investigation of *Bakuella*, *Anteholosticha*, and *Caudiholosticha* (Protista, Ciliophora, Hypotrichia) based on three-gene sequences. *J. Eukaryot. Microbiol.*, 62:391–399.

Lynn, D. H. 2008. The ciliated protozoa: Characterization, classification, and guide to the literature, 3rd ed. Springer, New York. p. 1–605.

Lynn, D. H. & Small, E. B. 2002. Phylum Ciliophora Doflein, 1901. *In:* Lee, J. J., Leedale, G. G. & Bradbury, P. C. (eds.), The Illustrated Guide to the Protozoa, 2nd ed. Allen Press Inc., Lawrence, KS. p. 371–656.

Medlin, L., Elwood, H. J., Stickel, S. & Sogin, M. L. 1988. The characterization of enzymatically amplified eukaryotes 16S-like ribosomal RNA coding regions. *Gene*, 71:491–500.

Miller, M. A., Pfeiffer, W. & Schwartz, T. 2010. Creating the CIPRES Science Gateway for inference of large phylogenetic trees. *In:* Proceedings of the Gateway Computing Environments Workshop (GCE), 14 Nov. New Orleans, LA. p. 1–8.

Nylander, J. A. 2004. MrModeltest, version 2.2. Evolutionary Biology Centre, Uppsala University, Uppsala.

Paiva, T. S. & Silva-Neto, I. D. 2005. *Deviata estevesi* sp. n. (Ciliophora: Spirotrichea), a new ciliate protist from a restinga lagoon in Rio de Janeiro, Brazil. *Acta Protozool.*, 44:351–362.

Paiva, T. S. & Silva-Neto, I. D. 2009. Morphology and divisional morphogenesis of *Nudiamphisiella interrupta* Foissner, Agatha & Berger, 2002 (Ciliophora: Stichotrichia) based on a Brazilian strain. *Eur. J. Protistol.*, 45:271–280.

Ronquist, F. & Huelsenbeck, J. P. 2003. MRBAYES 3: Bayesian phylogenetic inference under mixed models. *Bioinformatics*, 19:1572–1574.

Shao, C., Chen, L., Pan, Y., Warren, A. & Miao, M. 2014a. Morphology and phylogenetic position of the oxytrichid ciliates, *Urosoma salmastra* (Dragesco and Dragesco-Kerneis, 1986) Berger, 1999 and *U. karinae sinense* nov. sspec. (Ciliophora, Hypotrichia). *Eur. J. Protistol.*, 50:593–605.

Shao, C., Li, L., Zhang, Q., Song, W. & Berger, H. 2014b. Molecular phylogeny and ontogeny of a new ciliate genus, *Paracladotricha salina* n. g., n. sp. (Ciliophora, Hypotrichia). *J. Eukaryot. Microbiol.*, 61:371–380.

Shao, C., Lu, X. & Ma, H. 2015. A general overview of the typical 18 frontal-ventral-transverse cirri Oxytrichidae *s. l.* genera (Ciliophora, Hypotrichia). *J. Ocean Univ. China*, 14:522–532.

Singh, J. & Kamra, K. 2015. Molecular phylogeny of *Urosomoida agilis*, and new combinations: *Hemiurosomoida longa* gen. nov., comb. nov., and *Heterourosomoida lanceolata* gen. nov., comb. nov. (Ciliophora, Hypotricha). *Eur. J. Protistol.*, 51:55–65.

Siqueira-Castro, I. C. V., Paiva, T. S. & Silva-Neto, I. D. 2009. Morphology of *Parastrongylidium estevesi* comb. nov. and *Deviata brasiliensis* sp. nov. (Ciliophora: Stichotrichia) from a sewage treatment plant in Rio de Janeiro, Brazil. *Zoologia*, 26:774–786.

Spakova, T., Pristas, P. & Javorsky, P. 2014. Telomere repeats and macronuclear DNA organization in the soil ciliate *Kahliella matisi* (Ciliophora, Hypotricha). *Eur. J. Protistol.*, 50:231–235.

Stamatakis, A. 2014. RAxML version 8: a tool for phylogenetic analysis and post-analysis of large phylogenies. *Bioinformatics*. doi: 10.1093/bioinformatics/btu033.

Tamura, K., Dudley, J., Nei, M. & Kumar, S. 2007. MEGA 4: molecular evolutionary genetics analysis (MEGA) software ver. 4.0. *Mol. Biol. Evol.*, 24:1596–1599.

Wang, P., Gao, F., Huang, J., Strüder-Kypke, M. & Yi, Z. 2015. A case study to estimate the applicability of secondary structures of SSU-rRNA gene in taxonomy and phylogenetic analyses of ciliates. *Zool. Scr.*, 44:574–585.

Wilbert, N. 1975. Eine verbesserte Technik der Protargolimprägnation für Ciliaten. *Mikrokosmos*, 64:171–179. (in German).

Yi, Z. & Song, W. 2011. Evolution of the order Urostylida (Protozoa, Ciliophora): new hypotheses based on multi-gene information and identification of localized incongruence. *PLoS One*, 6: e17471. doi: 10.1371/journal.pone.0017471.

Zhao, X., Gao, S., Fan, Y., Strueder-Kypke, M. & Huang, J. 2015. Phylogenetic framework of the systematically confused *Anteholosticha-Holosticha* complex (Ciliophora, Hypotrichia) based on multigene analysis. *Mol. Phylogenet. Evol.*, 91:238–247.